Cardio-protective effects of pentraxin 3 produced from bone marrow-derived cells against ischemia/reperfusion injury

学位論文

Cardio-protective effects of pentraxin 3 produced from bone marrow-derived cells against ischemia/reperfusion injury

(骨髄由来細胞からの pentraxin 3 産生は心筋虚血再灌流傷害において保護的役割を果たす)

福島県立医科大学大学院医学研究科循環血液病態情報学分野専攻

清水　竹史

Cardio-protective effects of pentraxin 3 produced from bone marrow-derived cells against ischemia/reperfusion injury

Takeshi Shimizu[1], Satoshi Suzuki[1], Akihiko Sato[1], Yuichi Nakamura[1], Kazuhiko Ikeda[1], Shu-ichi Saitoh[1], Shingen Misaka[2], Tetsuro Shishido[3], Isao Kubota[3] and Yasuchika Takeishi[1]

[1]Department of Cardiology and Hematology, Fukushima Medical University, Fukushima, Japan

[2]Department of Pharmacology, Fukushima Medical University, Fukushima, Japan

[3]First Department of Internal Medicine, Yamagata University School of Medicine, Yamagata, Japan

Total words: 3486 words

Figures and Tables: 7 figures

Address for correspondence: Yasuchika Takeishi, MD, PhD

Department of Cardiology and Hematology

Fukushima Medical University

1 Hikarigaoka, Fukushima, 960-1295, Japan

Tel: 024-547-1190, Fax: 024-548-1821

E-mail: takeishi@fmu.ac.jp

Abstract

Background: Inflammation is one of major mechanisms contributing to the pathogenesis of myocardial ischemia/reperfusion (I/R) injury. Pentraxin 3 (PTX3), produced in response to inflammatory signals, acts as a humoral arm of the innate immunity. Here we investigated the role of PTX3 produced from bone marrow-derived cells in myocardial I/R injury using PTX3-deficient (PTX3KO) mice.

Methods and Results: PTX3KO mice and wild-type littermate (WT) mice were lethally irradiated and injected with bone marrow (BM) cells, generating four types of mice ($WT^{WT\text{-}BM}$, $WT^{PTX3KO\text{-}BM}$, $PTX3KO^{WT\text{-}BM}$ and $PTX3KO^{PTX3KO\text{-}BM}$). Six weeks after BM transplantation, the myocardial I/R procedure (45 minutes of left descending coronary artery ligation followed by 48 hours of reperfusion) was performed. Infarct size was greater in WT and PTX3KO mice with BM from PTX3KO donor ($WT^{PTX3KO\text{-}BM}$ and $PTX3KO^{PTX3KO\text{-}BM}$) compared with WT and PTX3KO mice with BM from WT donor ($WT^{WT\text{-}BM}$ and $PTX3KO^{WT\text{-}BM}$). Localization of PTX3 was observed in neutrophils and macrophages in WT and PTX3KO mice with BM from WT donor ($WT^{WT\text{-}BM}$ and $PTX3KO^{WT\text{-}BM}$), while only in endothelial cells in WT mice with BM from PTX3KO donor ($WT^{PTX3KO\text{-}BM}$). Infiltration of neutrophils and generation of reactive oxygen species (ROS) at ischemic border zones were greater in PTX3KO mice with BM from

PTX3KO donor ($PTX3KO^{PTX3KO\text{-}BM}$) than PTX3KO mice with BM from WT donor ($PTX3KO^{WT\text{-}BM}$). Plasma levels and cardiac expressions of interleukin-6 were higher in PTX3KO mice with BM from PTX3KO donor ($PTX3KO^{PTX3KO\text{-}BM}$) than PTX3KO mice with BM from WT donor ($PTX3KO^{WT\text{-}BM}$). However, no significant differences in infarct size, infiltration of neutrophils, generation of ROS and plasma and cardiac levels of interleukin-6 were observed between WT and PTX3KO mice with BM from WT donor and between WT and PTX3KO mice with BM from PTX3KO donor. These results indicated that the lack of PTX3 produced from BM-derived cells, and not from cardiac resident cells, exacerbated myocardial injury after I/R.

Conclusion: PTX3 produced from bone marrow-derived cells plays a crucial role in cardiac protection against myocardial I/R injury by attenuating infiltration of neutrophils, generation of ROS and inflammatory cytokine.

Key words:

Pentraxin 3, inflammation, ischemia/reperfusion, neutrophil, reactive oxygen species

1. Introduction

Although coronary artery reperfusion is currently the most effective therapy for acute myocardial infarction, the process of restoring blood flow to the ischemic myocardium itself can induce myocardial damages, also known as myocardial ischemia/reperfusion (I/R) injury. Lethal reperfusion injury, one of the different clinical manifestations of this paradoxical phenomenon and characterized as irreversible cell death, contains several potential mechanisms [1]. Inflammation is one of major mediators contributing to the pathogenesis of lethal reperfusion injury, including a rapid increase in cytokines and congregation of leukocytes in the injured myocardial region [2]. Neutrophils and monocytes are drawn into the infarct zone by chemoattractants and migrate into myocardial tissue during the first 24 hours of myocardial I/R. Monocytes subsequently give rise to reparative macrophages, thereby entering the resolution phase. These two phases (inflammatory and resolution phase) are essential for infarct healing [3]. However, in the pathogenesis of I/R injury, neutrophils release degradative enzymes and reactive oxygen species (ROS) leading to irreversible myocardial damage, which is a detrimental aspect of inflammatory response [4].

Pentraxin 3 (PTX3) belongs to the pentraxin superfamily and is an essential component of the humoral arm of innate immunity. PTX3 is expressed by various cell

types such as myeloid dendritic cells, neutrophils, macrophages, endothelial cells, fibroblasts and smooth muscle cells among others [5]. PTX3 expression is rapidly induced by several stimuli including inflammatory cytokines, Toll-like receptor agonists, and microbial moieties, with different signaling pathways depending on cell type and/or stimuli (e.g., NF-κB pathway in the acute myocardial ischemia model, c-Jun N-terminal kinase pathway in lung epithelial cells, and PI3K/Akt pathway in endothelial cells). Physiological functions of PTX3 are associated with the recognition and binding to different ligands; PTX3 modulates complement pathways by binding with complement component C1q, supports clearance of recognized pathogens by opsonization or phagocytosis, and inhibits leukocyte recruitment by interacting with P-selectin [6].

Several reports have described the cardiovascular protective [7,8] or detrimental [9] effects of PTX3 using genetically manipulated mice, indicating that PTX3 is potentially associated with the immunoinflammatory response observed in several cardiovascular diseases. Salio *et al.* [7] have revealed a cardio-protective role of PTX3 in myocardial I/R mouse model. In that report, they also elucidated that PTX3, which was expressed and/or produced in both leukocytes and cardiac resident cells, suppressed the no-reflow phenomenon and leukocyte infiltration in myocardial I/R injury. However, the origins of PTX3 functioning for protection of myocardium was

unclear.

In this study, we investigated the role of PTX3 produced from bone marrow-derived cells in myocardial I/R injury using PTX3 deficient mice.

2. Material and Methods

2.1. Animals and Ethics statement

PTX3-deficient (PTX3KO) mice and wild-type littermate (WT) mice (C57BL/6, male) were used for the experiments. PTX3KO mice were generated as previously described [10]. All experimental procedures were performed according to the animal welfare regulations of Fukushima Medical University, and the study protocol was approved by the Fukushima Medical University Animal Research Committee. The investigations conformed to the *Guidelines for the Care and Use of Laboratory Animals* published by the US National Institutes of Health (NIH publication, 8th Edition, 2011).

2.2. Bone Marrow Transplantation

PTX3KO and WT mice between 10 and 12 weeks of age were lightly anesthetized by titrating isoflurane (0.5-1.5%) and sacrificed via cervical dislocation. Whole bone marrow (BM) cells were harvested by flushing femurs with phosphate-buffered saline

(PBS), as previously reported [11]. The cells were washed twice with PBS and diluted to 5.0×10^6 cell/200 μL with saline. The recipient mice (8 weeks of age) were lethally irradiated with a total dose of 9 Gy and were injected with BM cells through the tail vein. Using this protocol, we produced four types of BM transplantation mice: WT-BM to WT recipient mice ($WT^{WT\text{-}BM}$), PTX3KO-BM to WT recipient mice ($WT^{PTX3KO\text{-}BM}$), WT-BM to PTX3KO recipient mice ($PTX3KO^{WT\text{-}BM}$), and PTX3KO-BM to PTX3KO recipient mice ($PTX3KO^{PTX3KO\text{-}BM}$). To confirm the engraftment of donor BM cells in the recipients, we extracted DNA from white blood cells and analyzed the genotypes. Blood samples were obtained from the retro-orbital plexus of recipient mice 6 weeks after BM transplantation, and DNA was isolated using the QIAamp DNA Mini Kit (Qiagen, Valencia, CA) according to the manufacturer's instructions. PCR was performed and reconstitution of the BM was verified. The following three primers were used at the same time, as previously reported [10]: 5'-AGCAATGCACCTCCCTGCGAT-3', 5'-CTGCTCTTTACTGAAGGCTC-3' and 5'-TCCTCGGTGGGATGAAGTCCA-3'. PCR products of 124 bp were obtained for WT, $WT^{WT\text{-}BM}$ and $PTX3KO^{WT\text{-}BM}$ mice, and 300 bp for PTX3KO, $WT^{PTX3KO\text{-}BM}$ and $PTX3KO^{PTX3KO\text{-}BM}$ mice (Figure 1).

2.3. Myocardial ischemia and reperfusion

After confirming BM reconstitution, mice were intubated with a 20-gauge polyethylene catheter under general anesthesia (0.25 mg/g of body weight, tribromoethanol) and positive-pressure ventilated with a rodent ventilator (Shinano Manufacturing, Tokyo, Japan). The hearts were exposed by left thoracotomy, and myocardial infarction was produced by suture occlusion of the left anterior descending coronary artery (LAD) over a silicon tube. After 45 minutes of ischemia, the tube and suture were removed to permit reperfusion. The heart was repositioned in the chest, and the chest wall was closed with a silk suture.

2.4. Assessment of infarct size

Forty-eight hours after reperfusion, the LAD was occluded again at the same position, and 1% Evans blue was injected via the inferior vena cava. The heart was then excised and sliced transversely into five to six sections which were incubated with 1.5% triphenyltetrazolium chloride (TTC) for 30 minutes at 37°C. The area lacking Evans blue staining was regarded as the area at risk (AAR), and the white-colored (TTC-negative) area within the AAR was considered the infarct area. The AAR was expressed as a percentage of the left ventricular mass (AAR/LV), and the infarct area

was expressed as a percentage of the AAR (infarct area/AAR). Area quantification was performed using Image J Software (NIH, Bethesda, MD).

2.5. Immunohistochemistry

For immunohistochemistry, the heart was excised 48 hours after I/R and immediately fixed with 4% paraformaldehyde and embedded in paraffin. After deparaffinization, the 5 μm thick sections were treated with 0.3% H_2O_2 in methanol for 30 minutes and digested with 100 mg/ml proteinase K in 0.05 mol/l Tris-HCl (pH 7.6) for 10 minutes at room temperature. After incubating with 5% skim milk, the sections were reacted with rat anti-mouse GR-1 antibody (eBioscience, San Diego, CA) at 4°C overnight to identify neutrophils at the risk area. The sections were then treated with horseradish peroxidase conjugated anti-rat IgG (Abcam, Cambridge, MA) followed by coloration with 3,3'-diaminobenzidine (Nichirei Biosciences, Inc., Tokyo, Japan) and counterstained with hematoxylin. Quantitative assessment of infiltrated neutrophils in the area at risk was performed by counting the number of positive cells in five different fields (1 mm^2) of the ischemic border zones. The border zone was defined as surviving cardiomyocytes that were in close contact with coagulative necrotic tissue, which was identified in sections of hematoxylin-eosin staining [12]. All measurements were

performed in a double-blind manner by two independent researchers.

For double immunofluorescence, the heart was excised 48 hours after I/R, embedded in the OCT compound (Tissue-Tek; Miles Laboratories, Elkhart, IN), then frozen in liquid nitrogen. The 8 μm thick sections were incubated with mouse anti-human PTX3 antibody (Perseus Proteomics Inc., Tokyo, Japan) simultaneously with rat anti-mouse GR-1 antibody (R&D Systems, Minneapolis, MN) for neutrophil, rat anti-mouse F4/80 antibody (Santa Cruz Biotechnology, Inc., Santa Cruz, CA) for macrophage, or goat anti-mouse CD31 (Santa Cruz Biotechnology) for endothelial cells at 4°C overnight. The anti-PTX3 reaction was developed in green (Alexa® Fluor 488 conjugated goat anti-mouse antibody; Cell Signaling Technology, Danvers, MA), GR-1 and F4/80 in red (Alexa® Fluor 594 conjugated rabbit anti-rat antibody; Molecular Probes, Eugene, OR) and CD31 also in red (Alexa® Fluor 594 conjugated donkey anti-goat antibody; Molecular Probes). The samples were observed using fluorescence microscopy (Olympus IX71, OLYMPUS Optical Co., Tokyo, Japan) after nuclear counterstaining with 4′,6-diamidino-2-phenylindole dihydrochloride (DAPI; Sigma-Aldrich, St.Louis, MO).

2.6. Enzyme-linked immunosorbent assay

Blood samples were collected from the retro-orbital plexus into the plasma separation tube at 24 hours after I/R and immediately centrifuged. Proteins were extracted from the snap-frozen left ventricle, which was excised at 24 hours after I/R with ice-cold lysis buffer, as previously reported [13]. The protein concentrations in the myocardial samples were determined using a protein assay (Bio-Rad Laboratories, Inc., Hercules, CA). The levels of interleukin-6 (IL-6) were assessed using the Mouse IL-6 ELISA Kit (RayBiotech, Inc., Norcross, GA) according to the manufacturer's instructions.

2.7. Assay of reactive oxygen species

The excised heart tissue 48 hours after I/R was immediately frozen in liquid nitrogen with OCT compound (Tissue-Tek) and sectioned at 8-μm thickness. The section was incubated with 5 μmol/l dihydroethidium (DHE; Sigma-Aldrich) at 37°C for 30 minutes in the dark. The fluorescent images were acquired using a fluorescence microscope (Olympus IX71, OLYMPUS Optical Co.) and the mean DHE fluorescence intensity of cardiomyocytes in the ischemic border areas, which of five randomly selected fields in each section, was quantitated with Image J Software (NIH).

Oxidative DNA damage in the myocardium was evaluated by 8-hydroxy-2'-deoxyguanosine (8-OHdG) immunostaining. After deparaffinization, the sections were

treated with 0.3% H_2O_2 in methanol for 30 minutes at room temperature, and boiled in sodium citrate (pH 6.0) by a microwave for 10 minutes. After incubating with 5% skim milk, the sections were reacted with anti-8-OHdG monoclonal antibody (clone N45.1, Japan Institute for the Control of Aging, Fukuroi, Japan) for one hour at room temperature in a humidity chamber, followed by staining with peroxidase-labeled secondary antibodies (Histofine Simple Stain Mouse MAX PO, Nichirei Biosciences, Inc.) and 3,3'-diaminobenzidine (Nichirei Biosciences, Inc.). The sections were then counterstained with hematoxylin.

For co-staining with DHE and ROS-generating cells, frozen sections were incubated with mouse anti-α actinin antibody (Sigma-Aldrich) for cardiomyocyte, rabbit anti-mouse CD31 (Santa Cruz Biotechnology) for vascular endothelial cells and rabbit anti-S100A4 antibody (Abcam) for fibroblast. The primary antibody reactions were developed in green (Alexa® Fluor 488 conjugated goat anti-mouse antibody; Cell Signaling Technology, and Alexa® Fluor 488 conjugated goat anti-rabbit antibody; Abcam), followed by counterstaining with DAPI and DHE staining as described above.

2.8. Ultra performance liquid chromatography

Dihydroethidium oxidation generates at least two fluorescent products;

2-hydroxyeyhidium, which is more specific for superoxide, and ethidium, which reflects H_2O_2-dependent pathways involving metal proteins [14]. We performed ultra performance liquid chromatography (UPLC) to separate and quantify these products and to estimate superoxide in the heart tissue after I/R [15]. The excised heart tissue 48 hours after I/R was immediately cut into 20 mg from left ventricular apex and incubated with Krebs-HEPES buffer containing 50 μM DHE at 37°C for 30 minutes. The heart tissues were then washed of DHE in Krebs-HEPES buffer, subsequently placed in 300 μl of cold methanol and homogenized. The solution was exsiccated by nitrogen gas, dissolved in 100 μl of 0.2% formic acid, and filtered (0.22 μm). The filtrate was then analyzed by UPLC as described below.

Separation of 2-hydroxyethidium, ethidium and DHE was performed using a Waters AQUITY UPLC H-class system with a AQUITY BEH C18 column (particle size 1.7 μm, ϕ 2.1×50 mm, Waters, Milford, MA) at 40°C. The samples were separated using an isocratic mobile phase consisting of 0.2% formic acid and acetonitrile (80:20, v/v) at a flow rate of 0.5 ml/min. DHE was monitored by ultraviolet absorption at 355 nm, and 2-hydroxyethidium was monitored by fluorescence detection at 480 nm (excitation) and 580 nm (emission). Generation of 2-hydroxyethidium was expressed as a ratio of integrated peak area per DHE consumed (initial DHE concentration minus

remaining DHE).

2.9. Statistical analysis

All results were distributed normally and expressed as mean ± standard error (S.E.). Statistical significance was evaluated using one-way analysis of variance (ANOVA) for comparisons among four groups, followed by multiple comparisons with the Tukey test. A *P* value of less than 0.05 was considered to be statistically significant. These analyses were performed using a statistical software package (SPSS ver. 21.0, IBM, Armonk, NY).

3. Results

3.1. Enlargement of infarct size after myocardial I/R by the lack of PTX3 from bone marrow-derived cells

To investigate whether PTX3 produced from BM-derived cells contributes to myocardial I/R injury, the myocardial I/R procedure was performed on four types of BM transplantation mice. Although no difference was observed in AAR/LV among the four groups (Figure 2A), the infarct area/AAR was significantly greater in $PTX3KO^{PTX3KO\text{-}BM}$ than in $WT^{WT\text{-}BM}$ (73.5 ± 2.4 vs. 49.3 ± 3.2, $P<0.01$) (Figure 2B). In

comparison of the same recipient types, infarct area/AAR was greater in $WT^{PTX3KO\text{-}BM}$ than in $WT^{WT\text{-}BM}$ (62.8 ± 3.7 vs. 49.3 ± 3.2%, $P<0.05$), and greater in $PTX3KO^{PTX3KO\text{-}BM}$ than in $PTX3KO^{WT\text{-}BM}$ (73.5 ± 2.4 vs. 57.0 ± 3.4%, $P<0.01$). No significant difference was observed between $WT^{WT\text{-}BM}$ and $PTX3KO^{WT\text{-}BM}$ ($P=0.43$).

3.2. PTX3 expression in neutrophils, macrophages and endothelial cells

We next assessed the cellular distribution of PTX3 by double immunofluorescence of PTX3 and neutrophils (anti-GR-1 antibody), macrophages (anti-F4/80 antibody) or endothelial cells (anti-CD31 antibody) in the ischemic myocardium. In $WT^{WT\text{-}BM}$ mice, PTX3 was localized in neutrophils, macrophages, and endothelial cells, but not in the cardiomyocytes (Figure 3A). In $WT^{PTX3KO\text{-}BM}$ mice, PTX3 was localized only in endothelial cells (Figure 3B). However, in $PTX3KO^{WT\text{-}BM}$ mice, PTX3 was localized in neutrophils and macrophages, but not in endothelial cells (Figure 3C). PTX3 expression was not identified in $PTX3KO^{PTX3KO\text{-}BM}$ mice (Figure 3D).

3.3. Increment of neutrophil infiltration and interleukin-6 expression after myocardial I/R by the lack of PTX3 from bone marrow-derived cells

It has been reported that neutrophils contribute to the myocardial I/R injury, and the

extent of infarct size after myocardial I/R is correlated with an increase in the population of accumulated neutrophils [16]. Therefore, to compare the infiltration of neutrophils into ischemic myocardium in each type of mice, immunohistochemical analysis using anti-GR-1 antibody was performed (Figure 4). GR-1 positive cells in the ischemic border zone were greater in $PTX3KO^{PTX3KO\text{-}BM}$ than in $WT^{WT\text{-}BM}$ and $PTX3KO^{WT\text{-}BM}$ (467.2 ± 34.1 vs. 312.5 ± 31.7 and 298.2 ± 25.2 /mm^2, P<0.01). No significant deference was observed between $WT^{WT\text{-}BM}$ and $PTX3KO^{WT\text{-}BM}$ (P=0.98)

To investigate whether inflammatory cytokines are involved in the increment of myocardial I/R injury in $PTX3KO^{PTX3KO\text{-}BM}$ and $WT^{PTX3KO\text{-}BM}$ mice, we assessed plasma and myocardial levels of interleukin-6 (IL-6) at 24 hours after reperfusion (Figure 5). IL-6 was significantly higher in $PTX3KO^{PTX3KO\text{-}BM}$ compared with $WT^{WT\text{-}BM}$ and $PTX3KO^{WT\text{-}BM}$ in both plasma (0.80 ± 0.27 vs. 0.15 ± 0.03 and 0.09 ± 0.01 ng/ml, P<0.05) and myocardial levels (14.8 ± 3.6 vs. 6.6 ± 0.8 and 5.9 ± 0.9 pg/mg protein, P<0.05), while no significant difference was observed between $WT^{WT\text{-}BM}$ and $PTX3KO^{WT\text{-}BM}$ (P=0.86).

3.4. Increment of oxidative stress after myocardial I/R by the lack of PTX3 from bone marrow-derived cells

Reactive oxygen species are greatly increased in the post-ischemic heart and serve as a central mechanism of myocardial I/R injury [17]. We evaluated cardiac ROS generation by DHE fluorescence (Figure 6A). The ROS generation in the ischemic border zones at 48 hours of reperfusion was higher in $PTX3KO^{PTX3KO\text{-}BM}$ and $WT^{PTX3KO\text{-}BM}$ than in $WT^{WT\text{-}BM}$ (28.7 ± 2.1 and 21.8 ± 4.6 vs. 12.0 ± 1.8, $P<0.01$ and $P<0.05$, respectively), which also was lower in $PTX3KO^{WT\text{-}BM}$ than in $PTX3KO^{PTX3KO\text{-}BM}$ (16.4 ± 3.2 vs. 28.7 ± 2.1, $P<0.05$). No significant difference was observed between $WT^{WT\text{-}BM}$ and $PTX3KO^{WT\text{-}BM}$ ($P=0.52$).

Oxidative DNA damage in the reperfused myocardium was evaluated by 8-OHdG immunostaining. The 8-OHdG positive nuclei were observed in ischemic cardiomyocytes (Figure 6B), and a ratio of 8-OHdG positive nuclei/total nuclei in ischemic border zones was higher in $PTX3KO^{PTX3KO\text{-}BM}$ and $WT^{PTX3KO\text{-}BM}$ than in $WT^{WT\text{-}BM}$ (48.3 ± 2.4 and 44.3 ± 2.2 vs. $25.8 \pm 2.2\%$, $P<0.01$) and lower in $PTX3KO^{WT\text{-}BM}$ than in $PTX3KO^{PTX3KO\text{-}BM}$ (33.5 ± 1.7 vs. $48.3 \pm 2.4\%$, $P<0.01$). No significant difference was observed between $WT^{WT\text{-}BM}$ and $PTX3KO^{WT\text{-}BM}$ ($P=0.46$).

We also measured 2-hydroxyethidium (2OH-E), which is formed in the reaction of DHE with superoxide, by UPLC (Fig 6C). Peak integral area of 2OH-E per consumed DHE was higher in $PTX3KO^{PTX3KO\text{-}BM}$ than in $WT^{WT\text{-}BM}$ (907.4 ± 39.3 vs. 530.4 ± 87.1

μVsec/μM, P<0.05). In comparison of the same recipient types, superoxide generation was greater in $WT^{PTX3KO\text{-}BM}$ than in $WT^{WT\text{-}BM}$ (840.3 ± 48.3 vs. 530.4 ± 87.1 μVsec/μM, $P<0.05$), and greater in $PTX3KO^{PTX3KO\text{-}BM}$ than in $PTX3KO^{WT\text{-}BM}$ (907.4 ± 39.3 vs. 578.9 ± 116.7 μVsec/μM, $P<0.05$). No significant difference was observed between $WT^{WT\text{-}BM}$ and $PTX3KO^{WT\text{-}BM}$ ($P=0.97$) or $WT^{PTX3KO\text{-}BM}$ and $PTX3KO^{PTX3KO\text{-}BM}$ ($P=0.93$).

3.5. Differences of ROS generation by the lack of PTX3 from bone marrow-derived cells appeared in cardiomyocytes, but not in endothelial cells or fibroblasts.

To examine potential mechanism of increased generation of ROS in mice with BM from PTX3KO donor mice ($WT^{PTX3KO\text{-}BM}$ and $PTX3KO^{PTX3KO\text{-}BM}$), we performed DHE staining subsequent to immunofluorescence of cardiomyocytes (anti-α actinin antibody), vascular endothelial cells (anti-CD31 antibody) and fibroblasts (anti-S100A4 antibody) (Figure 7).

DHE fluorescence intensity of myocardium was higher in mice with BM from PTX3KO donor mice ($WT^{PTX3KO\text{-}BM}$ and $PTX3KO^{PTX3KO\text{-}BM}$) than in mice with BM from WT donor mice ($WT^{WT\text{-}BM}$ and $PTX3KO^{WT\text{-}BM}$). On the other hand, DHE fluorescence intensity of endothelial cells and fibroblast did not differ among four types of mice,

indicating that PTX3 has not contributed to generation of ROS from endothelial cells and fibroblasts.

4. Discussion

This study demonstrates that deficiency of PTX3 produced from BM-derived cells, and not from cardiac resident cells, increases myocardial infarct size after I/R in mice. In addition, deficiency of PTX3 increases infiltration of neutrophils to the ischemic area, plasma levels and cardiac expressions of IL-6 and generation of ROS in the ischemic myocardium. Thus, these data indicate a cardio-protective role of PTX3 produced from BM-derived cells in myocardial I/R-induced inflammation and oxidative stress.

Although neutrophils play an important role in the healing process after myocardial infarction, they contribute to myocardial I/R injury by several mechanisms such as the release of ROS and proteases [18], embolization in microvessels leading to the no-reflow phenomenon [19], and the release of inflammatory mediators which amplifies further recruitment of neutrophils into the reperfused myocardium [20]. Accordingly, the extent of the infarct size in myocardial I/R injury has been correlated with an increase in the population of accumulated neutrophils [16]. Examinations for inhibiting neutrophil in animal models have been performed by a large number of

researchers using several approaches; leukocyte depletion, antibodies to adhesion molecules, anti-inflammatory agents, adenosine, protease inhibitors, and local anesthetics, showing enhanced recovery of contractile function or reduction of infarct size after I/R [4]. PTX3, which is stored in specific granules of neutrophils and released in response to inflammatory signals [21], has been reported to increase in the early phase of acute myocardial infarction [22]. Regarding the function of PTX3 in inflammation, Deban *et al.* [23] reported that PTX3 released from activated leukocytes functioned locally to attenuate neutrophil recruitment at the site of inflammation by binding selectively with P-selectin, which functions as a cell adhesion molecule on the surface of activated endothelial cells and platelets. According to this leukocyte modulating function of PTX3, lack of PTX3 have led to increased myocardial damage after I/R. Although Salio *et al.* [7] described larger infarct size and greater neutrophil infiltration in reperfused myocardium in PTX3-deficient mice compared with WT mice, the origins of PTX3 functioning for protection of myocardium was not obvious. Our experiments revealed that PTX3 produced from BM-derived leukocytes, but not from cardiac vascular endothelial cells, functioned to attenuate I/R-induced neutrophil infiltration and myocardial injury.

Reactive oxygen species are produced in myocardial I/R, and several reports

demonstrated that inhibiting formation of ROS could reduce infarct size [24]. Three major enzyme pathways were identified as the source of ROS production in I/R injury: (1) xanthine oxidase, primarily within endothelial cells; (2) the mitochondrial electron transport chain, primarily from the cardiomyocytes; (3) NADPH oxidase, primarily with leukocytes and fibroblasts [17]. We have showed the lack of PTX3 produced from leukocytes induced increased ROS generation in the damaged myocardium after I/R, but not in vascular endothelial cells or fibroblasts. Although we could not exclude a direct link between PTX3 and generation of ROS in myocardium, our data indicate PTX3 participates in ROS reduction by attenuating their recruitment into reperfused myocardium. The increased generation of free radicals and oxidants from neutrophils by lack of PTX3 is not an only pathologic cause in myocardial I/R; larger magnitude of neutrophil infiltration leads to a greater degree of no-reflow phenomenon as Salio *et al.* [7] described, but it critically contributes to the increased damages of cardiomyocytes after I/R.

Future studies are required to explore the effects of anti-neutrophil and antioxidant therapy in this model to verify the results in this study, which is a limitation of the present study.

5. Conclusion

We demonstrated that PTX3 produced from bone marrow-derived cells inhibited infiltration of neutrophils and ROS generation at the ischemic myocardium, thereby resulting in the reduction of infarct size after ischemia-reperfusion.

Funding

This work was partly supported by a grant-in-aid for Scientific Research (No. 25870584) from the Japan Society for the Promotion of Science and grants-in-aid from the Japanese Ministry of Health, Labor and Welfare, Tokyo, Japan.

Conflict of Interest

All authors declare no conflict of interest.

Acknowledgements

We thank Dr. Mizuko Tanaka for her helpful comments regarding immunofluorescence, and Ms. Emiko Watanabe and Minae Takasaki for their excellent technical assistance.

References

1. Yellon DM, Hausenloy DJ. Myocardial Reperfusion Injury. N Engl J Med 2007; 357: 1121-1135.
2. Arslan F, de Kleijn DP, Timmers L, Doevendans PA, Pasterkamp G. Bridging innate immunity and myocardial ischemia/reperfusion injury: the search for therapeutic targets. Curr Pharm Des 2008; 14: 1205-1216.
3. Swirski FK, Nahrendorf M. Leukocyte behavior in atherosclerosis, myocardial infarction, and heart failure. Science 2013; 339: 161-166.
4. Vinten-Johansen J. Involvement of neutrophils in the pathogenesis of lethal myocardial reperfusion injury. Cardiovasc Res 2004; 61: 481-497.
5. Bottazzi B, Doni A, Garlanda C, Mantovani A. An integrated view of humoral innate immunity: pentraxins as a paradigm. Annu Rev Immunol 2010; 28: 157-183.
6. Moalli F, Jaillon S, Inforzato A, Sironi M, Bottazzi B, et al. Pathogen Recognition by the Long Pentraxin PTX3. J Biomed Biotechnol. 2011; 2011: 830421
7. Salio M, Chimenti S, De Anqelis N, Molla F, Maina V, et al. Cardioprotective Function of the Long Pentraxin PTX3 in Acute Myocardial Infarction. Circulation 2008; 117: 1055-1064.

8. Norata GD, Marchesi P, Pulakazhi Venu VK, Pasqualini F, Anselmo A, et al. Deficiency of the Long Pentraxin PTX3 Promotes Vascular Inflammation and Atherosclerosis. Circulation 2009; 120: 699-708.

9. Suzuki S, Shishido T, Funayama A, Netsu S, Ishino M, et al. Long pentraxin PTX3 exacerbates pressure overload-induced left ventricular dysfunction. PLosONE 2013; 8: e53133.

10. Garlanda C, Hirsch E, Bozza S, Salustri A, De Acetis M, et al. Non-redundant role of the long pentraxin PTX3 in anti-fungal innate immune response. Nature 2002; 420: 182-186.

11. Yajima N, Takahashi M, Morimoto H, Shiba Y, Takahashi Y, et al. Critical role of bone marrow apoptosis-associated speck-like protein, an inflammasome adaptor molecule, in neointimal formation after vascular injury in mice. Circulation 2008; 117: 3079-3087.

12. Morel S, Braunersreuther V, Chanson M, Bouis D, Rochemont V, et al. Endothelial Cx40 limits myocardial ischemia/reperfusion injury in mice. Cardiovasc Res. 2014; 102: 329-337.

13. Takeishi Y, Huang Q, Abe J, Glassman M, Che W, et al. Src and multiple MAP kinase activation in cardiac hypertrophy and congestive heart failure under chronic

pressure-overload: comparison with acute mechanical stretch. J Mol Cell Cardiol 2001; 33: 1637-1648.

14. Zhao H, Kalivendi S, Zhang H, Joseph J, Nithipaticom K, et al. Superoxide reacts with hydroethidine but forms a fluorescent product that is distinctly different from ethidium: potential implications in intracellular fluorescence detection of superoxide. Free Radic Biol Med 2003; 34: 1359-1368.
15. Fink B, Laude K, McCann L, Doughan A, Harrison DG, et al. Detection of intracellular superoxide formation in endothelial cells and intact tissues using dihydroethidium and an HPLC-based assay. Am J Physiol Cell Physiol. 2004; 287: C895-902.
16. Zhao ZQ, Velez DA, Wang NP, Hewan-Lowe KO, Nakamura M, et al. Progressively developed myocardial apoptotic cell death during late phase of reperfusion. Apoptosis 2001; 6: 279-290.
17. Zweier JL, Talukder MA, et al. The role of oxidants and free radicals in reperfusion injury. Cardiovasc Res 2006; 70: 181-190.
18. Albertine KH, Weyrich AS, Ma XL, Lefer DJ, Becker LC, et al. Quantification of neutrophil migration following myocardial ischemia and reperfusion in cats and dogs. J Leukoc Biol 1994; 55: 557-566.

19. Schmid-Schönbein GW. The damaging potential of leukocyte activation in the microcirculation. Angiology 1993; 44: 45-56.

20. Higo K, Sano J, Karasawa A, Kubo K. The novel thromboxane A2 receptor antagonist KW-3635 reduces infarct size in a canine model of coronary occlusion and reperfusion. Arch Int Pharmacodyn Ther 1993; 323: 32-49.

21. Jaillon S, Peri G, Delneste Y, Frémaux I, Doni A, et al. The humoral pattern recognition receptor PTX3 is stored in neutrophil granules and localizes in extracellular traps. J Exp Med 2007; 204: 793-804.

22. Maugeri N, Rovere-Querini P, Slavich M, Coppi G, Doni A, et al. Early and transient release of leukocyte pentraxin 3 during acute myocardial infarction. J Immunol 2011; 187: 970-979.

23. Deban L, Russo RC, Sironi M, Moalli F, Scanziani M, et al. Regulation of leukocyte recruitment by the long pentraxin PTX3. Nat Immunol 2010; 11: 328-334.

24. Dhalla NS, Elmoselhi AB, Hata T, Makino N. Status of myocardial antioxidants in ischemia-reperfusion injury. Cardiovasc Res 2000; 47: 446-456.

Figure legends

Figure 1. Analysis of chimeric mouse blood. PCR was performed with DNA extracted from white blood cells six weeks after bone marrow transplantation. PCR products of 124 bp were obtained for WT, $WT^{WT\text{-}BM}$ and $PTX3KO^{WT\text{-}BM}$, and 300 bp for PTX3KO, $WT^{PTX3KO\text{-}BM}$ and $PTX3KO^{PTX3KO\text{-}BM}$.

Figure 2. Enlargement of infarct size after myocardial I/R by the lack of PTX3 from bone marrow-derived cells. Quantitative measurement of AAR (Evans blue negative) relative to the area of the whole left ventricular transverse section (AAR/LV) and the infarct area (TTC negative) relative to AAR was performed in mice after 45 minutes of ischemia followed by 48 hours of reperfusion. Although no difference was observed in AAR/LV among the four groups (A), the infarct area/AAR was significantly greater in $PTX3KO^{PTX3KO\text{-}BM}$ than in $WT^{WT\text{-}BM}$. In comparison of the same recipient types, infarct area/AAR was greater in $WT^{PTX3KO\text{-}BM}$ than in $WT^{WT\text{-}BM}$, and greater in $PTX3KO^{PTX3KO\text{-}BM}$ than in $PTX3KO^{WT\text{-}BM}$ (B). Representative cross sections are shown below the corresponding bars. Each bar represents mean ± SE (n = 9-12). $^{*}P<0.05$ and $^{**}P<0.01$ vs. $WT^{WT\text{-}BM}$, $^{\#\#}P<0.01$ vs. $PTX3KO^{WT\text{-}BM}$. Data were analyzed

by one-way ANOVA followed by the Tukey test.

Figure 3. PTX3 expression in neutrophils, macrophages and endothelial cells after myocardial I/R. After 48 hours from reperfusion, the sections of the ischemic areas were analyzed by double-immunofluorescence staining with antibodies against PTX3 and GR-1 (neutrophils), F4/80 (macrophages) or CD31 (endothelial cells). PTX3 was localized in neutrophils and macrophages in $WT^{WT\text{-}BM}$ (A) and $PTX3KO^{WT\text{-}BM}$ (C), and endothelial cells in $WT^{WT\text{-}BM}$ (A) and $WT^{PTX3KO\text{-}BM}$ (B). PTX3 expression was not identified in $PTX3KO^{PTX3KO\text{-}BM}$ (D). Scale bars represent 10 μm in images of neutrophils and macrophages, 40 μm in endothelial cells.

Figure 4. Increment of neutrophil infiltration into the ischemic myocardium after myocardial I/R by the lack of PTX3 from bone marrow-derived cells. The sections of ischemic border zones, defined as surviving cardiomyocytes which were in close contact with coagulative necrotic tissue (A), were stained with anti-GR-1 antibody to visualize infiltration of neutrophils and quantitative assessment of infiltrated neutrophils was performed (B). GR-1 positive cells in the ischemic border zones were greater in $PTX3KO^{PTX3KO\text{-}BM}$ than in $WT^{WT\text{-}BM}$ and $PTX3KO^{WT\text{-}BM}$. Data are expressed as mean ±

SE (n = 5 for each). $^{**}P<0.01$ vs. $WT^{WT\text{-}BM}$, $^{\#\#}P<0.01$ vs $PTX3KO^{WT\text{-}BM}$. Data were analyzed by one-way ANOVA followed by the Tukey test.

Figure 5. Increment of plasma and cardiac expression of IL-6 in myocardial I/R injury by the lack of PTX3 from bone marrow-derived cells. (A), Plasma levels of IL-6 at 24 hours of reperfusion were assessed. IL-6 level was significantly higher in $PTX3KO^{PTX3KO\text{-}BM}$ compared with $WT^{WT\text{-}BM}$ and $PTX3KO^{WT\text{-}BM}$. (B), Myocardial levels of IL-6 were assessed. IL-6 level was significantly higher in $PTX3KO^{PTX3KO\text{-}BM}$ compared with $WT^{WT\text{-}BM}$ and $PTX3KO^{WT\text{-}BM}$. Data are expressed as mean ± SE (n = 7 for each). $^{*}P<0.05$ vs. $WT^{WT\text{-}BM}$, $^{\#}P<0.05$ vs $PTX3KO^{WT\text{-}BM}$. Data were analyzed by one-way ANOVA followed by the Tukey test.

Figure 6. Increment of oxidative stress after myocardial I/R by the lack of PTX3 from bone marrow-derived cells. The sections of ischemic border zones were stained with DHE to visualize ROS levels of myocardium (A) and with anti 8-OHdG antibody to evaluate oxidative DNA damages (B). Relative fluorescence intensity was higher in $PTX3KO^{PTX3KO\text{-}BM}$ and $WT^{PTX3KO\text{-}BM}$ than in $WT^{WT\text{-}BM}$, and lower in $PTX3KO^{WT\text{-}BM}$ than in $PTX3KO^{PTX3KO\text{-}BM}$ (A). A ratio of 8-OHdG positive nuclei/total cells in

ischemic border areas was increased in PTX3KO$^{PTX3KO\text{-}BM}$ and WT$^{PTX3KO\text{-}BM}$ compared with WT$^{WT\text{-}BM}$, and lower in PTX3KO$^{WT\text{-}BM}$ compared with PTX3KO$^{PTX3KO\text{-}BM}$ (B). In the superoxide quantification by UPLC, peak integral area of 2-hydroxyethidium per DHE was higher in PTX3KO$^{PTX3KO\text{-}BM}$ and WT$^{PTX3KO\text{-}BM}$ compared with WT$^{WT\text{-}BM}$, and lower in PTX3KO$^{WT\text{-}BM}$ compared with PTX3KO$^{PTX3KO\text{-}BM}$ (C). Representative images are shown below the corresponding bars. Each bar represents mean ± SE (n = 5 for each (A) (B), and n = 8 for each (C)). $*P<0.05$ and $**P<0.01$ vs. WT$^{WT\text{-}BM}$, $^{\#}P<0.05$ vs. PTX3KO$^{WT\text{-}BM}$. Data were analyzed by one-way ANOVA followed by the Tukey test.

Figure 7. PTX3 affected ROS in cardiomyocytes, but not in vascular endothelial cells and fibroblasts. DHE fluorescence intensity of myocardium at ischemic border zone was higher in WT$^{PTX3KO\text{-}BM}$ and PTX3KO$^{PTX3KO\text{-}BM}$ than in WT$^{WT\text{-}BM}$ and PTX3KO$^{WT\text{-}BM}$. On the other hand, DHE fluorescence intensity of endothelial cells and fibroblasts did not differ among the four types of mice, indicating that PTX3 has not contributed to generation of ROS from endothelial cells and fibroblasts. Scale bars represent 10 μm.

Figure 1

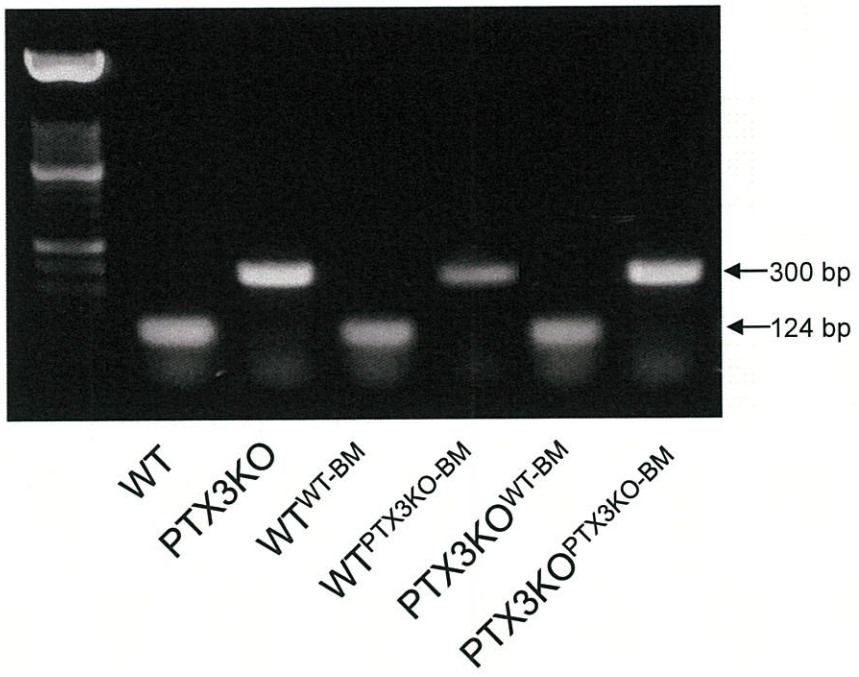
300 bp
124 bp
WT
PTX3KO
WT^WT-BM
WT^PTX3KO-BM
PTX3KO^WT-BM
PTX3KO^PTX3KO-BM

Figure 2

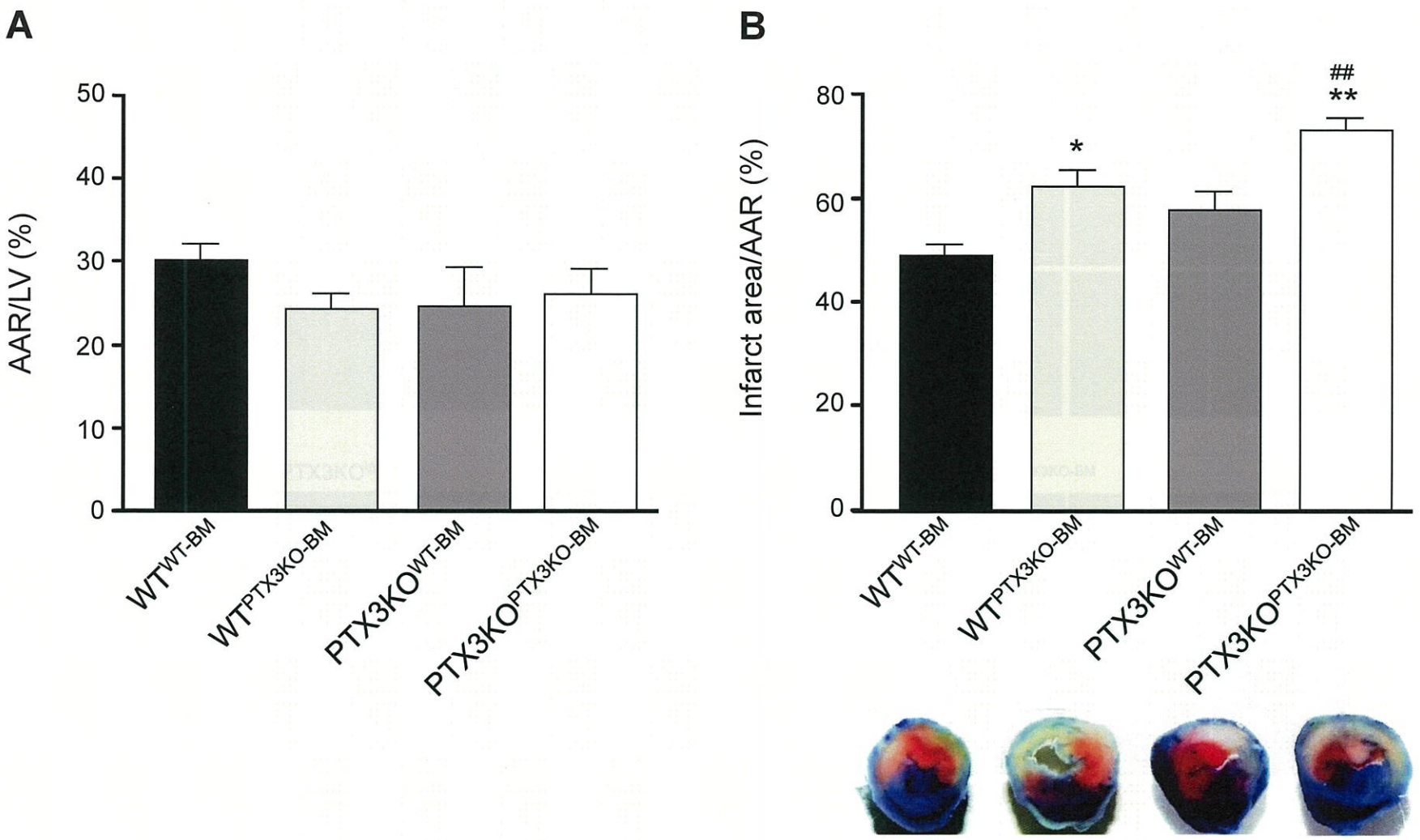
A
AAR/LV (%)
50
40
30
20
10
0
WTWT-BM
WTPTX3KO-BM
PTX3KOWT-BM
PTX3KOPTX3KO-BM
B
Infarct area/AAR (%)
80
60
40
20
0
*
##
**
WTWT-BM
WTPTX3KO-BM
PTX3KOWT-BM
PTX3KOPTX3KO-BM

Figure 3

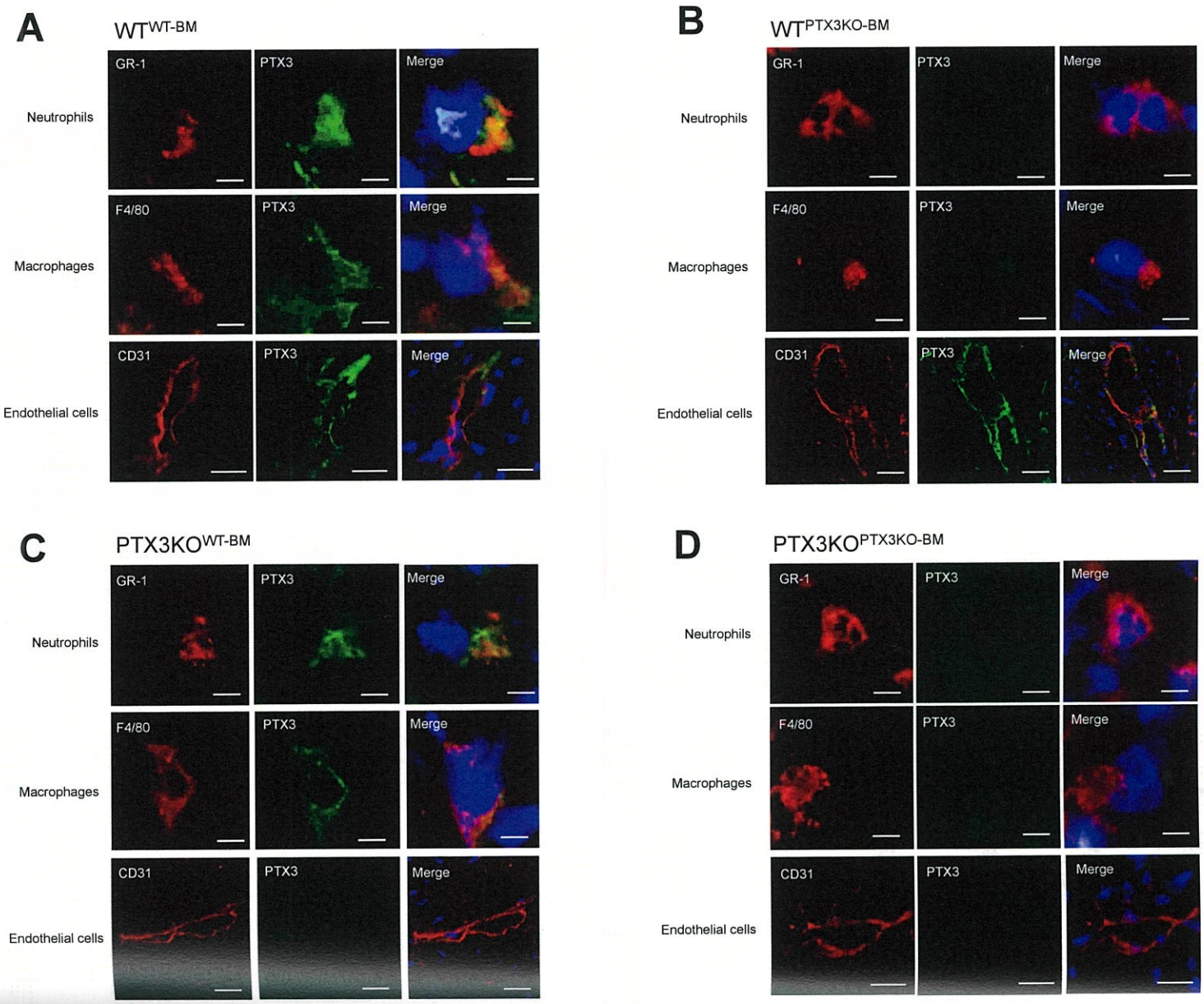
A
WT WT-BM
GR-1
PTX3
Merge
Neutrophils
F4/80
PTX3
Merge
Macrophages
CD31
PTX3
Merge
Endothelial cells
B
WT PTX3KO-BM
GR-1
PTX3
Merge
Neutrophils
F4/80
PTX3
Merge
Macrophages
CD31
PTX3
Merge
Endothelial cells
C
PTX3KO WT-BM
GR-1
PTX3
Merge
Neutrophils
F4/80
PTX3
Merge
Macrophages
CD31
PTX3
Merge
Endothelial cells
D
PTX3KO PTX3KO-BM
GR-1
PTX3
Merge
Neutrophils
F4/80
PTX3
Merge
Macrophages
CD31
PTX3
Merge
Endothelial cells

Figure 4

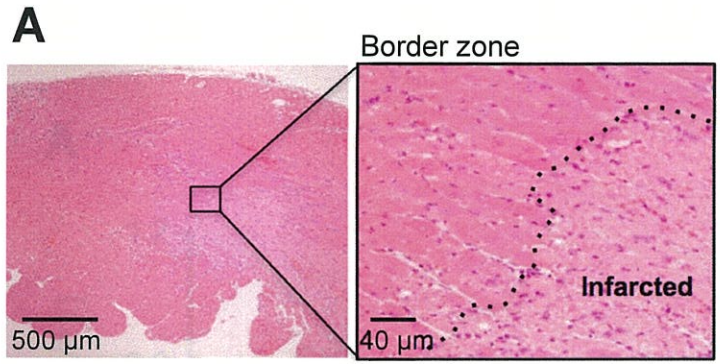
A
Border zone
Infarcted
500 μm
40 μm

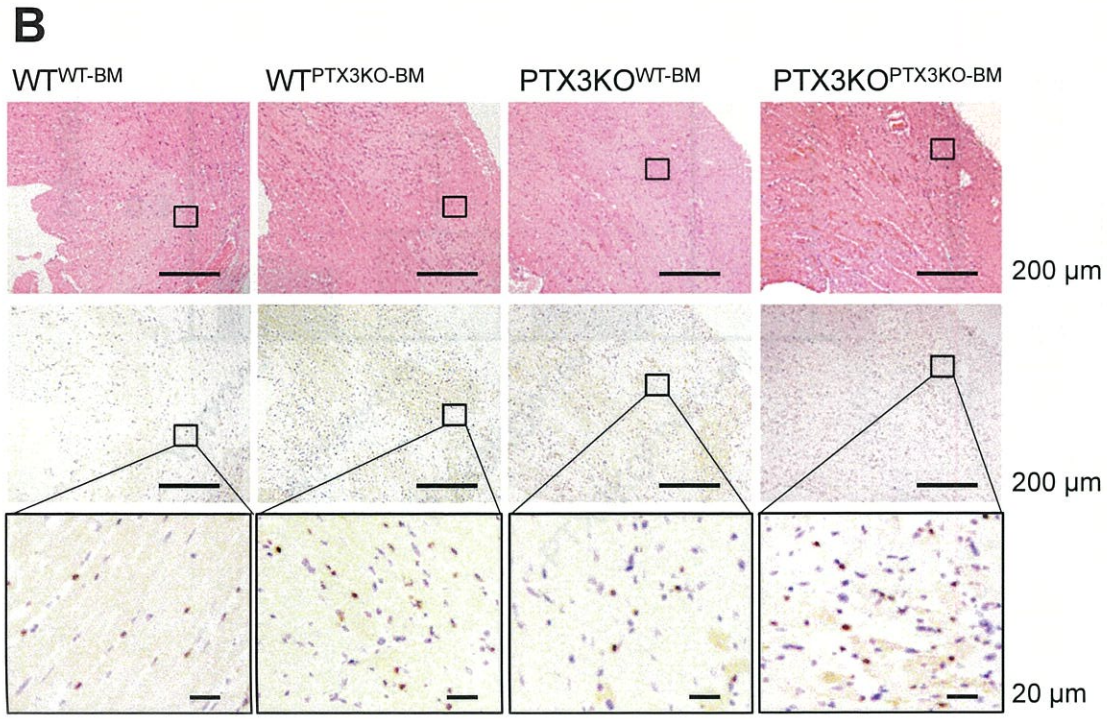
B
WT^WT-BM
WT^PTX3KO-BM
PTX3KO^WT-BM
PTX3KO^PTX3KO-BM
200 μm
200 μm
20 μm

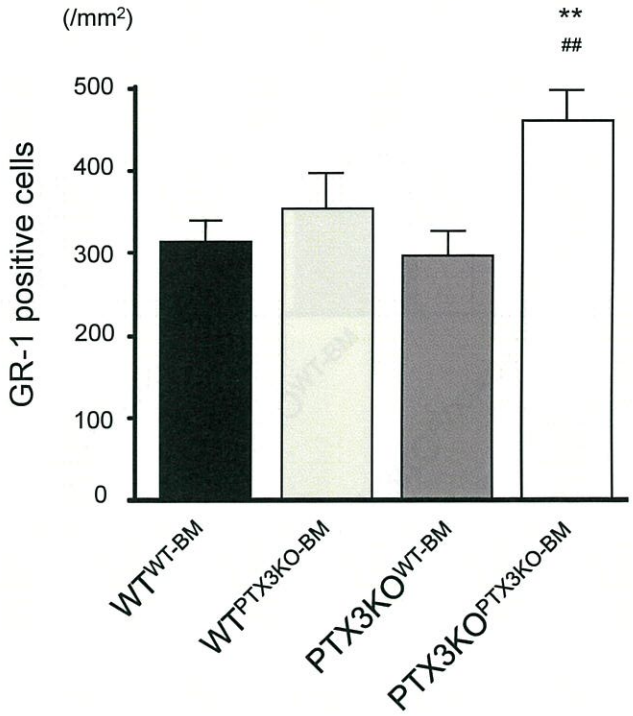
(/mm²)
**
##
GR-1 positive cells
500
400
300
200
100
0
WT^WT-BM
WT^PTX3KO-BM
PTX3KO^WT-BM
PTX3KO^PTX3KO-BM

Figure 5

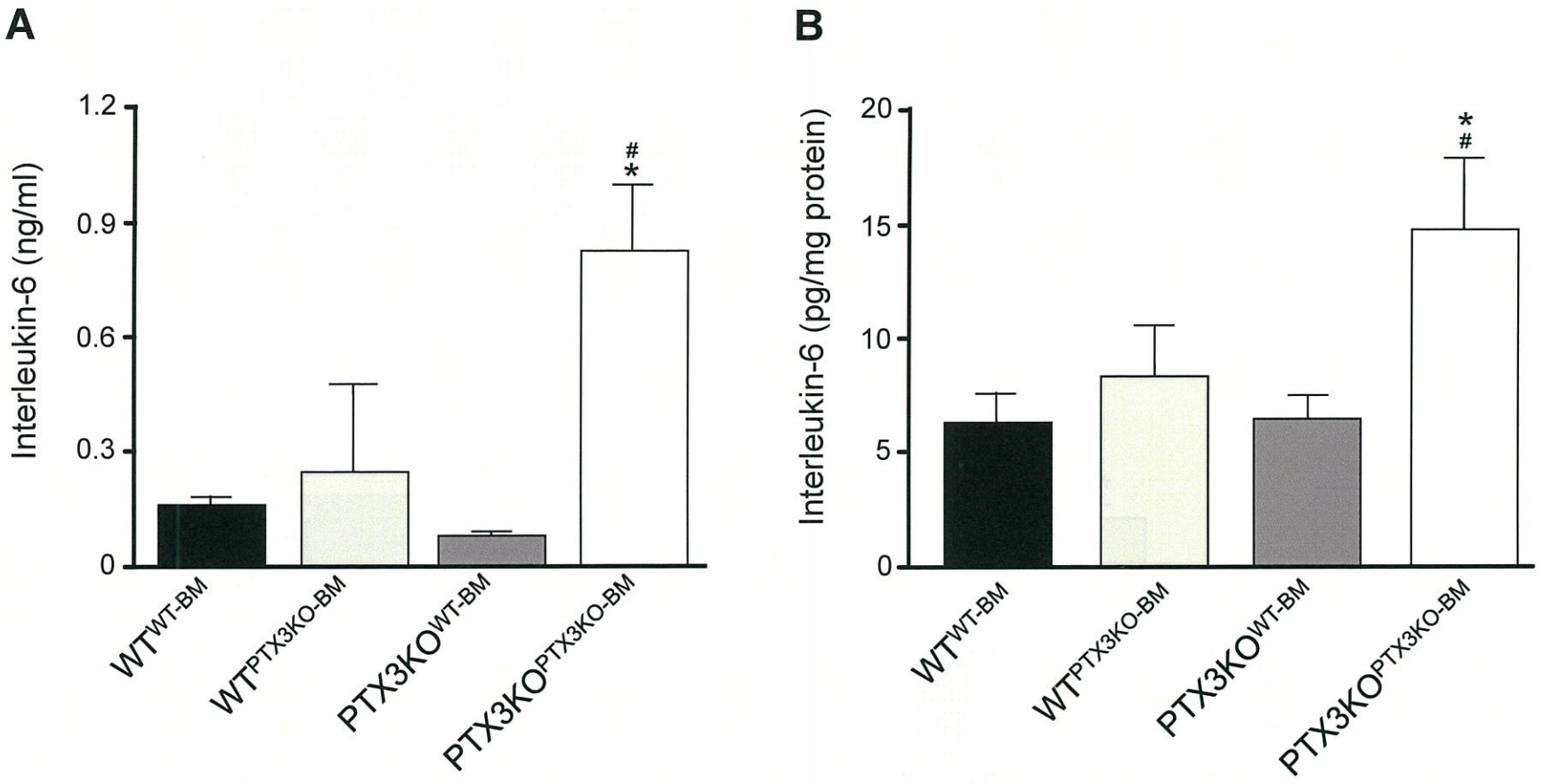
A
Interleukin-6 (ng/ml)
1.2
0.9
0.6
0.3
0
#
*
WT WT-BM
WT PTX3KO-BM
PTX3KO WT-BM
PTX3KO PTX3KO-BM
B
Interleukin-6 (pg/mg protein)
20
15
10
5
0
*
#
WT WT-BM
WT PTX3KO-BM
PTX3KO WT-BM
PTX3KO PTX3KO-BM

Figure 6

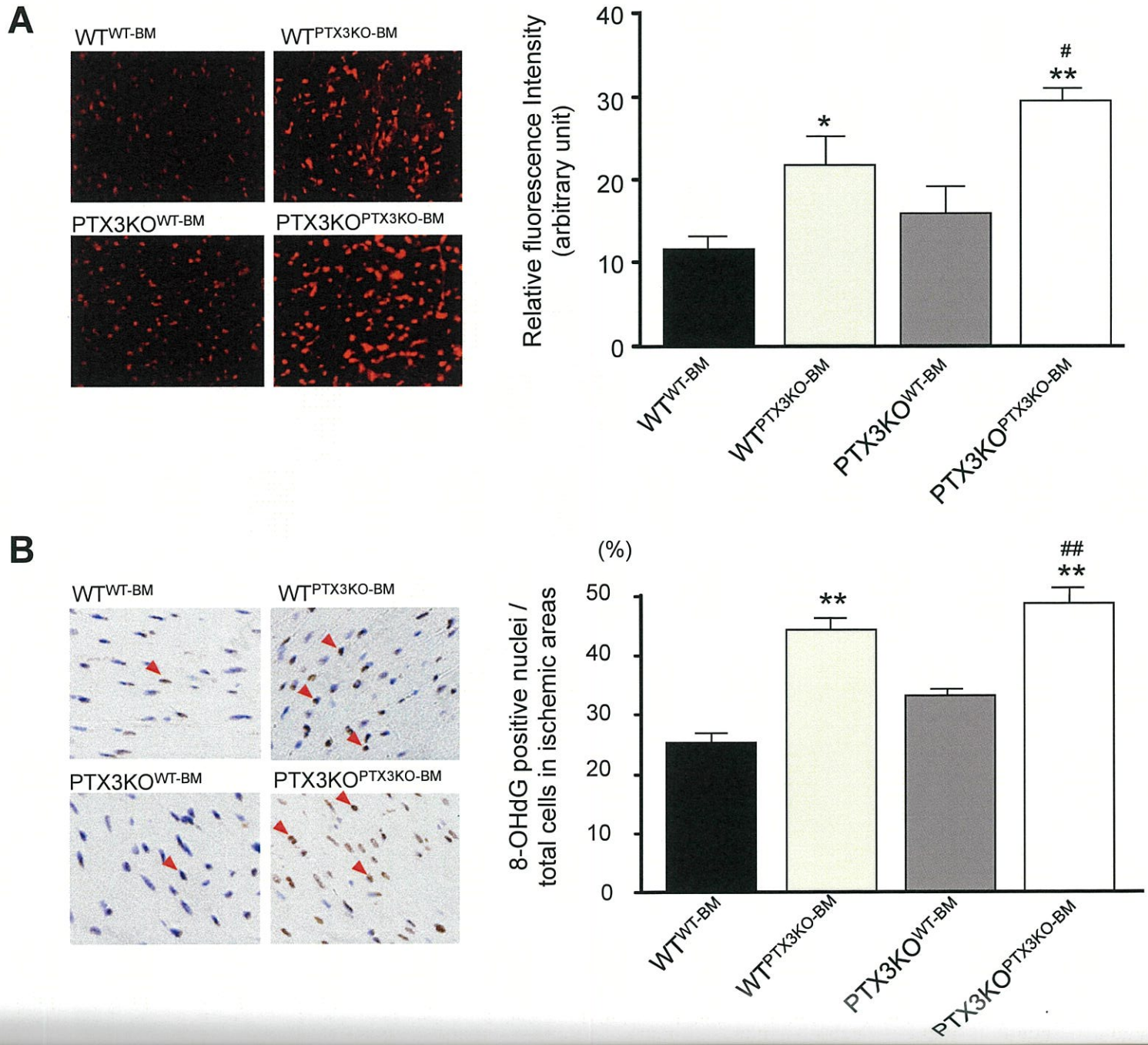
A
WT WT-BM
WT PTX3KO-BM
PTX3KO WT-BM
PTX3KO PTX3KO-BM
Relative fluorescence Intensity (arbitrary unit)
40
30
20
10
0
*
**
#
WT WT-BM
WT PTX3KO-BM
PTX3KO WT-BM
PTX3KO PTX3KO-BM
B
WT WT-BM
WT PTX3KO-BM
PTX3KO WT-BM
PTX3KO PTX3KO-BM
(%)
8-OHdG positive nuclei / total cells in ischemic areas
50
40
30
20
10
0
**
**
##
WT WT-BM
WT PTX3KO-BM
PTX3KO WT-BM
PTX3KO PTX3KO-BM

Figure 6

C

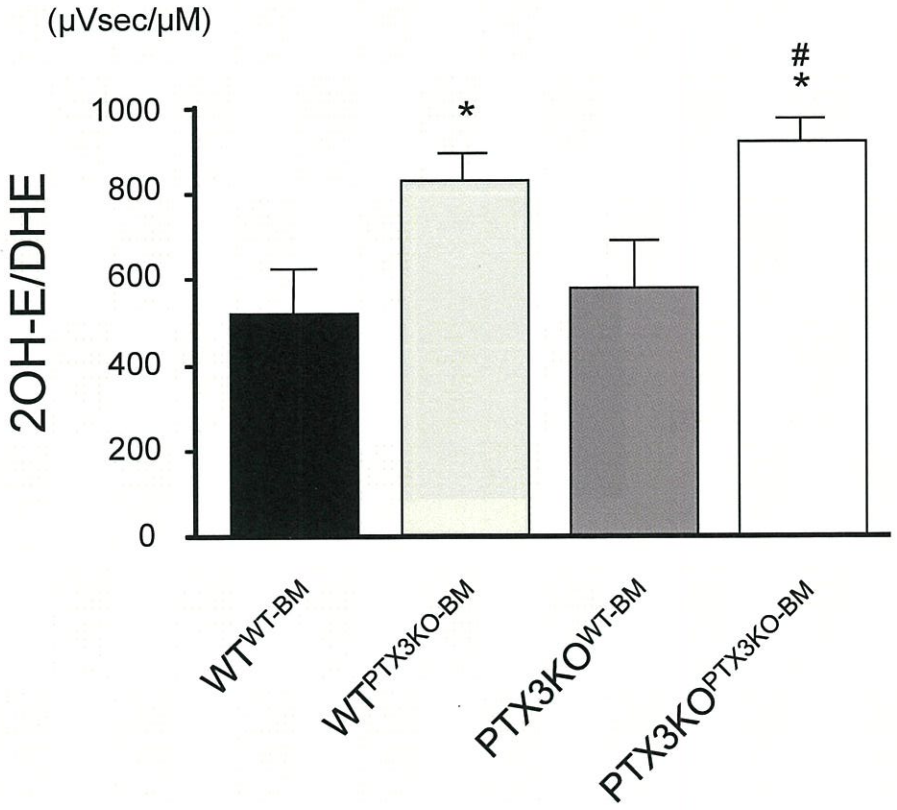
(μVsec/μM)
2OH-E/DHE
1000
800
600
400
200
0
*
#
*
WTWT-BM
WTPTX3KO-BM
PTX3KOWT-BM
PTX3KOPTX3KO-BM

Figure 7

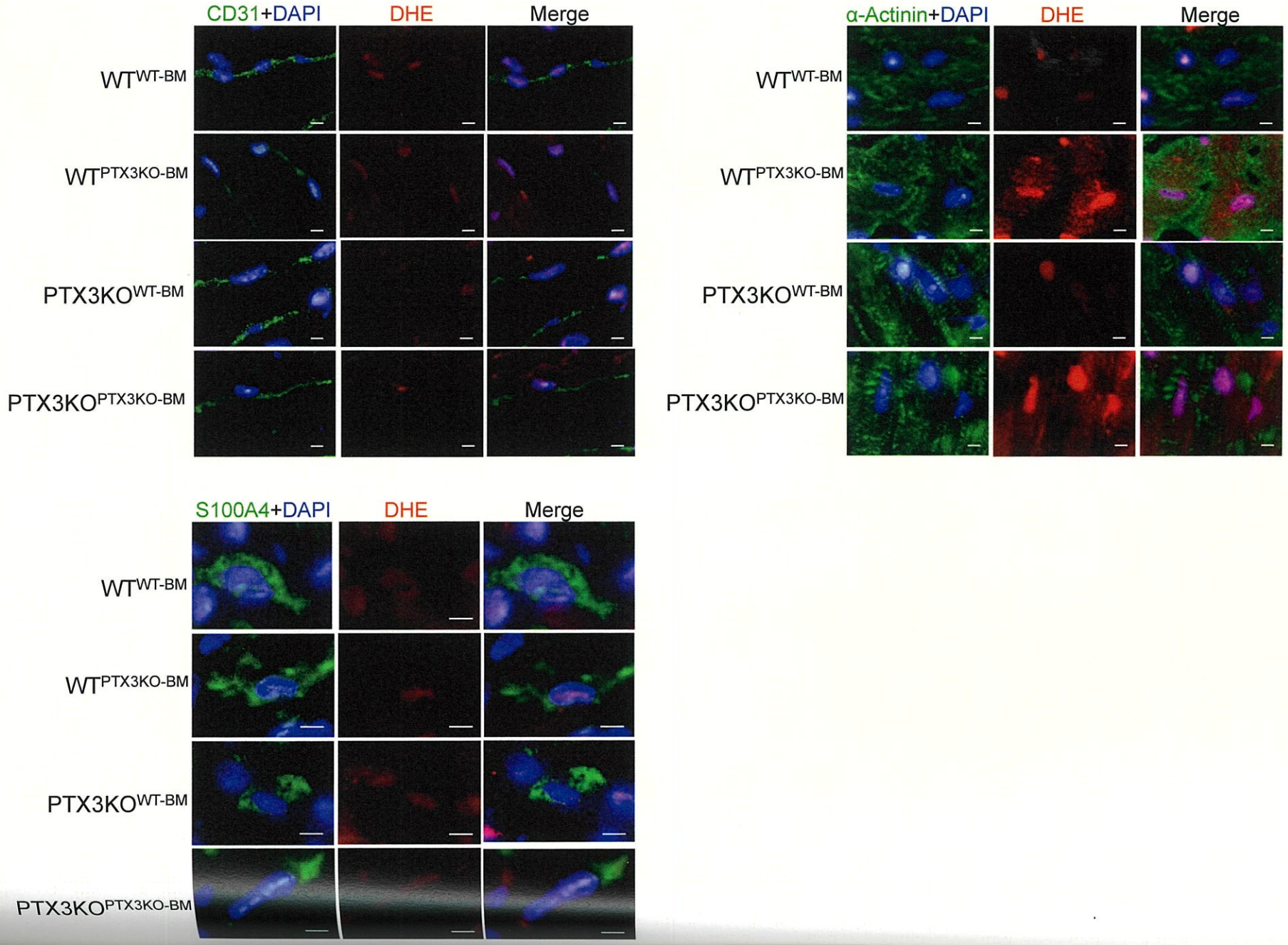
CD31+DAPI
DHE
Merge
WT^WT-BM
WT^PTX3KO-BM
PTX3KO^WT-BM
PTX3KO^PTX3KO-BM
α-Actinin+DAPI
DHE
Merge
WT^WT-BM
WT^PTX3KO-BM
PTX3KO^WT-BM
PTX3KO^PTX3KO-BM
S100A4+DAPI
DHE
Merge
WT^WT-BM
WT^PTX3KO-BM
PTX3KO^WT-BM
PTX3KO^PTX3KO-BM